Science and Technology Infusion Climate Bulletin
NOAA's National Weather Service
40th NOAA Annual Climate Diagnostics and Prediction Workshop
Denver, CO, 26-29 October 2015

Detection and Attribution of Extreme Temperature Using an Analogue-based Dynamical Adjustment Technique

Flavio Lehner[1], Clara Deser[1], Laurent Terray[2]
[1]*Climate and Global Dynamics Division, National Center for Atmospheric Research, Boulder, CO, USA*
[2]*Sciences de L'Univers au CERFACS, URA-1875, CERFACS/CNRS, Toulouse, France*

1. Introduction

Recent studies have highlighted the importance of internal variability in decadal trends and variability of regional-scale temperature and precipitation (Deser *et al.* 2012; Hawkins *et al.* 2015). Understanding and potentially reducing the uncertainties in climate change projections arising from internal variability has been a focal point of climate research over the last decade (Bindoff *et al.* 2013). The superposition of anthropogenically forced climate change with this unforced internal variability complicates attempts to detect and attribute climate change (Thompson *et al.* 2009). In the Northern Hemisphere mid to high latitudes, the stochastic variability of atmospheric circulation is a major contributor to this internal variability (Smoliak *et al.* 2015; Deser *et al.* 2015). Beyond decadal trends in temperature or precipitation, recent research has focused on diagnosing the driving factors behind individual extreme events, such as heat waves, cold snaps, or floods (Herring *et al.* 2015). It is therefore of interest to estimate the contribution of atmospheric circulation to a given trend or anomaly in temperature or precipitation.

Here we present a new method, based on constructed analogues, to estimate the contribution of atmospheric circulation to a given surface temperature anomaly. The details and an application to decadal temperature trends are described in Deser *et al.* 2015. The paper here is structured as follows. Section 2 summarizes the new method and introduces the data it is applied to. Section 3 illustrates how this method can be used to diagnose high temperature events. Section 4 summarizes these results and provides an outlook onto ongoing and future projects.

2. Data and methodology/experimental design

a. Dynamical adjustment of temperature

To estimate the contribution of atmospheric circulation to surface air temperature (SAT) changes, we apply a dynamical adjustment technique based on constructed circulation analogues. A full description of the methodology is given in Deser *et al.* 2015, of which we provide a summary here.

The method aims at empirically determining the component of SAT variability that arises solely from atmospheric circulation changes, characterized here by sea level pressure (SLP). This component is termed the 'dynamical contribution' to temperature variability. Subtracting the dynamical contribution from the raw field yields the residual, which is to first order an estimate of the 'thermodynamical contribution'.

In practice, for a given target month, *e.g.*, July 2015, we looking through all other available Julys in a given record, searching for Julys which have an analogues SLP pattern to the target month. The closest analogues are determined by finding the smallest Euclidean distance from the SLP pattern of the target month. Among the closest 80 analogues we randomly choose 50. An optimal linear combination of the 50 analogues is then computed that best fits the SLP pattern of the target month. Using the linear coefficients determined this way, we construct a SAT anomaly field that is defined as the optimal linear combination of the SAT anomalies associated with the SLP analogues. The process of randomly selecting 50 out of 80 analogues and constructing a best fit pattern is repeated 100 times to get an upper bound on the thermodynamically-induced internal variability. We then average over the 100 sets of SLP analogues and associated SAT anomalies to

Correspondence to: Flavio Lehner, Climate and Global Dynamics Division, National Center for Atmospheric Research, Boulder, CO; E-mail: flehner@ucar.edu.

arrive at a best estimate of dynamically induced SAT anomalies for the target pattern. This dynamic contribution can then be subtracted from the target SAT field, yielding a dynamically adjusted field. The whole procedure is applied analogously to all months available, so that eventually all monthly mean SAT fields in a given record are dynamically adjusted. Prior to the whole analysis, the SAT time series is detrended with a quadratic fit to remove the global warming signal (see Deser *et al.* 2015 for details). The dynamical adjustment is applied to the following model simulations and observational datasets.

b. Model simulations and observations

We use monthly mean output from the Large Ensemble with the fully coupled Community Earth System Model 1, hereafter CESM LE (Kay *et al.* 2015). The CESM LE is an ensemble of 30 simulations from 1920 to 2100, in which each simulation was started from slightly different atmospheric initial conditions, while using the same ocean initial conditions. In accordance with protocols from the Coupled Model Intercomparison Project 5 (CMIP5; Taylor *et al.* 2012), historical natural and anthropogenic forcing was applied from 1920 to 2005 and the Representative Concentration Pathway 8.5 (RCP 8.5) thereafter. Due to its size, the Large Ensemble allows us to sample internal variability in a robust manner, as will be shown in Section 3b.

For observations we use monthly mean SAT from MLOST (Vose *et al.* 2012) and SLP from the Twentieth Century Reanalysis (Compo *et al.* 2011).

3. Results

a. Application to observed high temperature events

We pick two examples from observations to illustrate the dynamical adjustment method: the exceptionally warm July over the US in 1980 and the exceptionally warm August over central Europe in 2003.

Fig. 1a shows the raw SAT anomaly of July 1980, relative to its 1951-1980 climatology, as well as the corresponding SLP. During this month, a strong and persistent heatwave took hold of large parts of the Midwestern US, with SAT anomalies of over 5°C. Fig. 1b shows the dynamical contribution to the SAT field in Fig. 1a as determined by the dynamical adjustment method. The SLP pattern in Fig. 1b is the analogue constructed from similar July SLP patterns in the observational record. There is good agreement of this pattern with the SLP pattern in Fig. 1a, indicating that the dynamical adjustment is successful in constructing analogues patterns (the residual/"error" is given in Fig. 1c). The SAT anomalies in Fig. 1b are then the constructed SAT field, *i.e.*, the SAT anomalies that typically go along

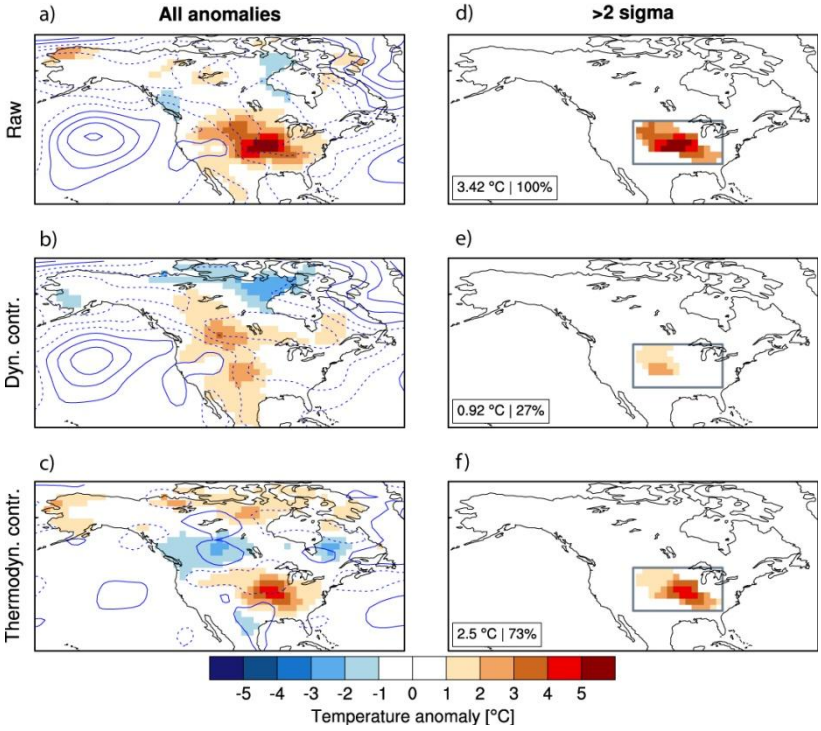

Fig. 1 (a) July 1980 surface air temperature (SAT; shading) and sea level pressure (SLP; contours, in 1 hPa increments starting at +/− 0.5 hPa) anomalies from their 1951-1980 climatology. (b) Dynamical contribution of constructed SLP pattern (contours) to SAT anomalies (shading). (c) Thermodynamic contribution to SAT anomalies (shading) and difference between true and constructed SLP anomalies (contours) as residual from subtracting (b) from (a). (d-f) Same as (a-c), but only SAT anomalies >2σ are shown. The spatial mean over the gray box is given in the bottom left corner with the fraction of the mean in panel (d).

with such a SLP pattern. Fig. 1c shows the SAT anomalies that remain after subtracting the dynamical contribution from the raw SAT anomaly (*i.e.*, Fig. 1a minus 1b), termed 'thermodynamical contribution'.

During this particular July (and preceding June; not shown), a strong high pressure system was positioned off and over the US west coast, deflecting eastwards-moving storms, thereby causing warm (and dry; not shown) conditions over the Great Plains (Fig. 1a). Indeed, the dynamical contribution suggests that such SLP patterns lead to elevated temperatures across most of the Great Plains (Fig. 1b). However, SLP did not contribute significantly to the heart of the warm anomaly just southwest of the Great Lakes. Indeed, most of the warm anomaly there seems to have been contributed by thermodynamic processes, related to the co-occurring drought (Fig. 1c).

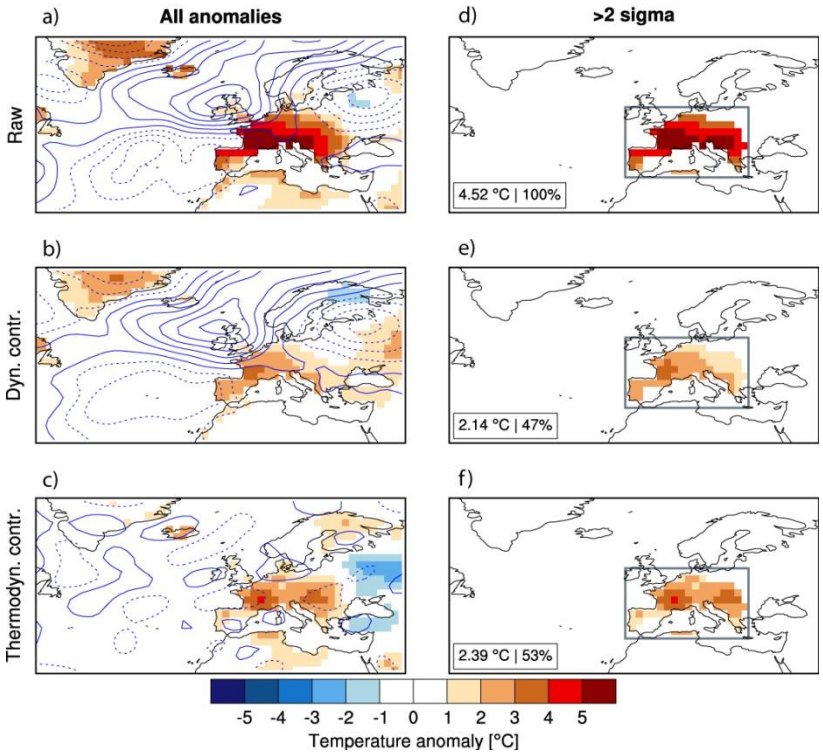

Fig. 2 Same as Fig. 1, but for August 2003 over Europe.

Fig. 1d-f show the same data as Fig. 1a-c, but only those regions where SAT anomalies were greater than two standard deviation (2σ) of their local 1951-1980 climatology (before calculating the climatology the data was detrended with a quadratic fit). The SAT anomaly averaged over the gray box is given in the bottom left corner. This depiction suggest that atmospheric dynamics, as described by SLP, only contributed 27% to the >2σ SAT anomaly of that month (Fig. 1e), while 73% can be attributed to thermodynamic processes. This is generally in line with understanding from other studies regarding this particular event (Wolfson and Atlas 1987; Lyon and Dole 1995). These studies suggest that while remote dynamical forcing was important in setting the stage for the heat wave, more local, thermodynamic effects, such as soil moisture feedbacks, controlled the amplitude and longevity of the heat wave throughout July.

The second example concerns the month of August during the 2003 summer heat wave in Europe (Fig. 2). In August 2003, a strong high pressure system positioned itself over central Europe, leading to a classical blocking situation. Anomalous high and low pressure North and South of the English Channel, respectively, shielded central Europe from any Atlantic disturbances (Fig. 2a). The dynamical adjustment method estimates that such a blocking typically creates about 2.14 °C of SAT anomaly (Fig. 2e), which constitutes only about 47% of the observed >2σ SAT anomaly. The remaining 53% of the temperature anomaly was likely made up by thermodynamic processes. Again, depleted soil moisture, arising from a dry spring, was found to having contributed substantially to this large thermodynamic contribution (Fischer *et al.* 2007).

b. Temporal evolution of dynamical contribution to temperature anomalies

After illustrating the dynamical adjustment on individual months, we aggregate this information over space and longer time periods and take the CESM LE into consideration (Fig. 3). To that end, we focus on >1σ SAT anomalies, as there are not enough >2σ SAT anomalies in observations to achieve robust aggregated results. First, we average across all >1σ SAT anomalies and their accompanying dynamic contributions in the domains (North America, 20-75°N, 170-50°W; and Europe, 35-75°N, 170°W-45°E). Second, we multiply this with the land fraction that these anomalies take up. This later quantity gives a sense

of SAT anomaly amplitude and spatial extent (hereafter called 'anomaly magnitude'). The following examples are based on boreal summer means (June-August).

In North America the period 1930-1940 (the "Dust Bowl" era) was marked by exceptional anomaly magnitudes, which are not reproduced by any of the ensemble members of CESM LE (Fig. 3a), indicating that the model is lacking a process or additional forcing that would be crucial for the generation of such anomaly magnitudes. Previous model studies found that specifying additional dust emissions from land use change and drought during that period improves the agreement with observations (Cook *et al.* 2008). Still, the dynamical adjustment suggests a significant contribution from dynamics during 1930-1940, originating from a persistent high pressure ridge over the Western US, as identified by other studies (Brönnimann *et al.* 2009). Averaged over the period 1920-1980 the partitioning between dynamic and thermodynamic contributions to >1σ anomaly magnitudes is about 50% each in both observations (47% vs. 53%) and CESM (50% vs. 50%). After 1980, the model's forced response (the ensemble mean) shows an increase in anomaly magnitudes, largely driven by an increase of the thermodynamic contribution, which constitutes the fingerprint of radiative forcing from increasing greenhouse gas concentrations.

The European domain is smaller and on average has a larger contribution from dynamics during 1920-1980 (57% in observations, 66% in CESM). After 1980, Europe shows a very similar behavior as North America with increasing anomaly magnitudes, mainly driven by an increase in the thermodynamic contribution. The summer of 2003 as a whole, taking into account June and July in addition to August (Fig. 2), shows a large thermodynamic contribution in observations.

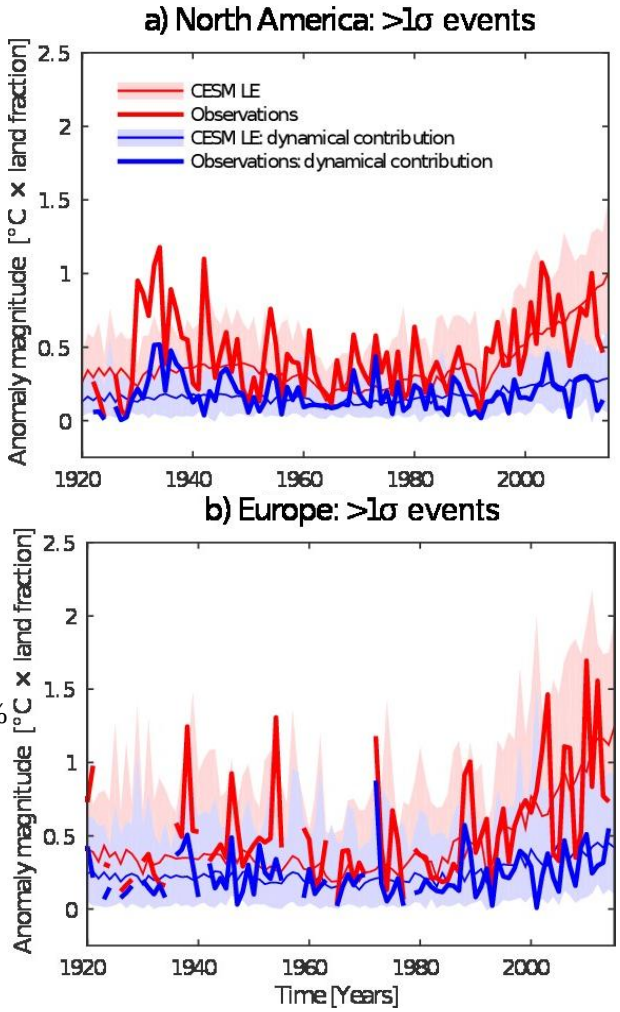

Fig. 3 Time series of anomaly magnitude of >1σ events, averaged from June through August (see text for details) for (a) North America and (b) Europe and the relative contribution from dynamics. Bold lines are observations, while thin lines and shading are the CESM LE ensemble mean and minimum-maximum range across the ensemble, respectively. Gaps in observations indicate that there occurred no >1σ event in that particular summer over the respective domain.

4. Summary and outlook

In this study we applied a new method that estimates the dynamically induced variability from a surface air temperature field using constructed circulation analogues (Deser *et al.* 2015). It is shown that the method can be used to diagnose drivers of a given temperature anomaly in observations, but also help to understand the dynamic and thermodynamic contributions to anthropogenically driven climate change in model simulations.

The CESM LE shows skill in reproducing the partitioning between dynamic and thermodynamic contributions of high summer temperatures as suggested by observations, namely about 50% each for the period prior to 1980 over North America. A notable exception is the Dust Bowl era, which in its amplitude and spatial extent is not reproduced by any of the CESM simulations.

Diagnosing other climate variables, such as precipitation, or events on shorter time scale, such as heat waves, constitute promising future avenues of this method.

References

Bindoff, N., and Coauthors, 2013: Detection and attribution of climate change: from global to regional. *Climate Change 2013: The Physical Science Basis. Contribution of Working Group I to the Fifth Assessment Report of the Intergovenermnetal Panel on Climate Change.*

Brönnimann, S., and Coauthors, 2009: Exceptional atmospheric circulation during the "Dust Bowl". *Geophys. Res. Lett.*, **36**, 1–6. doi:10.1029/2009GL037612.

Compo, G. P., and Coauthors, 2011: The Twentieth Century Reanalysis Project. *Q. J. R. Meteorol. Soc.*, **137**, 1–28. doi:10.1002/qj.776.

Cook, B. I., R. L. Miller, and R. Seager, 2008: Dust and sea surface temperature forcing of the 1930s "Dust Bowl" drought. *Geophys. Res. Lett.*, **35**, 1–5. doi:10.1029/2008GL033486.

Deser, C., R. Knutti, S. Solomon, and A. S. Phillips, 2012: Communication of the role of natural variability in future North American climate. *Nat. Clim. Chang.*, **2**, 775–779. doi:10.1038/nclimate1562.

——, L. Terray, and A. S. Phillips, 2016: Forced and internal components of winter air temperature trends over North America during the past 50 years: Mechanisms and implications. *J. Climate*, e-view. doi: 10.1175/JCLI-D-15-0304.1

Fischer, E. M., S. I. Seneviratne, P. L. Vidale, D. Lüthi, and C. Schär, 2007: Soil moisture-atmosphere interactions during the 2003 European summer heat wave. *J. Climate*, **20**, 5081–5099, doi:10.1175/JCLI4288.1.

Hawkins, E., R. S. Smith, J. M. Gregory, and D. A. Stainforth, 2015: Irreducible uncertainty in near-term climate projections. *Clim. Dyn.* doi:10.1007/s00382-015-2806-8.

Herring, S. C., M. P. Hoerling, J. P. Kossin, T. C. Peterson, and P. A. Stott, Eds., 2015: Explaining extreme events of 2014 from a climate perspective. *Bull. Amer. Meteor. Soc*., **96** (12), S1–S172.

Kay, J. E., and Coauthors, 2015: The Community Earth System Model (CESM) Large Ensemble Project: A community resource for studying climate change in the presence of internal climate variability. *Bull. Amer. Meteor. Soc.*, **96**, 1333–1349.

Lyon, B., and R. M. Dole, 1995: A diagnostic comparison of the 1980 and 1988 US summer heat wave-droughts. *J. Climate*, **8**, 1658–1675. doi:10.1175/1520-0442(1995)008<1658:ADCOTA>2.0.CO;2.

Smoliak, B. V., J. M. Wallace, P. Lin, and Q. Fu, 2015: Dynamical adjustment of the Northern Hemisphere surface air temperature field: Methodology and application to observations. *J. Climate*, **28**, 1613–1629. doi:10.1175/JCLI-D-14-00111.1.

Taylor, K. E., R. J. Stouffer, and G. a. Meehl, 2012: An overview of CMIP5 and the experiment design. *Bull. Am. Meteorol. Soc.*, **93**, 485–498. doi:10.1175/BAMS-D-11-00094.1.

Thompson, D. W. J., J. M. Wallace, P. D. Jones, and J. J. Kennedy, 2009: Identifying signatures of natural climate variability in time series of global-mean surface temperature: Methodology and insights. *J. Climate*, **22**, 6120–6141. doi:10.1175/2009JCLI3089.1.

Vose, R. S., and Coauthors, 2012: NOAA's Merged Land–Ocean Surface Temperature Analysis. *Bull. Am. Meteorol. Soc.*, **93,** 1677–1685. doi:10.1175/BAMS-D-11-00241.1.

Wolfson, N., and R. Atlas, 1987: Numerical experiments related to the summer 1980 US heat wave. *Mon. Weather Rev.*, **115**, 1345-1357.